The Plant Cell, Vol. 29: 2882–2894, November 2017, www.plantcell.org © 2017 ASPB.

ZEITLUPE Contributes to a Thermoresponsive Protein Quality Control System in Arabidopsis

Kyung-Eun Gil,[a] Woe-Yeon Kim,[b] Hyo-Jun Lee,[a] Mohammad Faisal,[c] Quaiser Saquib,[d] Abdulrahman A. Alatar,[c] and Chung-Mo Park[a,e,1]

[a] Department of Chemistry, Seoul National University, Seoul 08825, Korea
[b] Institute of Agriculture and Life Sciences, Gyeongsang National University, Jinju 52828, Korea
[c] Department of Botany and Microbiology, College of Science, King Saud University, Riyadh 11451, Saudi Arabia
[d] Department of Zoology, College of Science, King Saud University, Riyadh 11451, Saudi Arabia
[e] Plant Genomics and Breeding Institute, Seoul National University, Seoul 08826, Korea

ORCID IDs: 0000-0003-2470-4056 (K.-E.G.); 0000-0002-8176-1527 (M.F.); 0000-0001-8841-8361 (C.-M.P.)

Cellular proteins undergo denaturation and oxidative damage under heat stress, forming insoluble aggregates that are toxic to cells. Plants possess versatile mechanisms to deal with insoluble protein aggregates. Denatured proteins are either renatured to their native conformations or removed from cellular compartments; these processes are often referred to as protein quality control. Heat shock proteins (HSPs) act as molecular chaperones that assist in the renaturation-degradation process. However, how protein aggregates are cleared from cells in plants is largely unknown. Here, we demonstrate that heat-induced protein aggregates are removed by a protein quality control system that includes the ZEITLUPE (ZTL) E3 ubiquitin ligase, a central circadian clock component in *Arabidopsis thaliana*. ZTL mediates the polyubiquitination of aggregated proteins, which leads to proteasomal degradation and enhances the thermotolerance of plants growing at high temperatures. The ZTL-defective *ztl-105* mutant exhibited reduced thermotolerance, which was accompanied by a decline in polyubiquitination but an increase in protein aggregate formation. ZTL and its interacting partner HSP90 were cofractionated with insoluble aggregates under heat stress, indicating that ZTL contributes to the thermoresponsive protein quality control machinery. Notably, the circadian clock was hypersensitive to heat in *ztl-105*. We propose that ZTL-mediated protein quality control contributes to the thermal stability of the circadian clock.

INTRODUCTION

Protein misfolding occurs during both normal cellular folding processes and under environmental and oxidative stress conditions. The accumulation of misfolded proteins leads to the formation of insoluble aggregates, which are toxic to protein homeostasis and cellular integrity in eukaryotes (McClellan et al., 2005). Versatile protein quality control mechanisms have evolved to deal with misfolded proteins and insoluble protein aggregates by either facilitating their refolding into native conformations or directing their degradation via diverse ubiquitin-proteasome pathways (Finka and Goloubinoff, 2013).

Controlled protein degradation via the ubiquitin-proteasome pathway is initiated when molecular chaperones, such as HEAT SHOCK PROTEIN70 (HSP70) and HSP90, fail to refold misfolded proteins into their native state (McClellan et al., 2005; Finka and Goloubinoff, 2013). The molecular chaperones recognize the hydrophobic parts of misfolded proteins and recruit distinct ubiquitin ligase enzymes to the protein aggregates, each forming a ubiquitin-proteasome apparatus that determines which parts of the aggregates are to be removed (McClellan et al., 2005). For example, the C-terminal domain of C terminus of HSC70-interacting protein (CHIP) plays an important role in eliminating cytosolic protein aggregates by selectively ubiquitinating HSP70-associated misfolded proteins in animals and plants (Zhou et al., 2014; Lee et al., 2009). In addition, the E3 ubiquitin ligase CULLIN5 triggers polyubiquitination-mediated proteasomal degradation of HSP90 clients in animal cells (Samant et al., 2014).

HSP90 is a key molecular chaperone that is abundant and highly conserved in eukaryotes (McClellan et al., 2005; Krishna and Gloor, 2001). This protein plays essential roles in signal transduction pathways and cell cycle control by enhancing cell viability under stressful conditions (Krishna and Gloor, 2001; Finka et al., 2015). *Arabidopsis thaliana* contains seven HSP90 members localized to distinct subcellular compartments (Krishna and Gloor, 2001). These proteins are functionally associated with the maturation and stabilization processes of numerous regulatory proteins that function in diverse signaling networks. HSP90 interacts with cochaperone SGT1, stabilizing the immune-sensing nucleotide binding domain and leucine-rich repeat proteins (Shirasu, 2009). HSP90 also plays a role in buffering genetic variation and ensuring developmental stability (Sangster et al., 2008; Sangster and Queitsch, 2005).

The molecular chaperone HSP90 also participates in cellular responses to environmental stress, and its roles in thermal adaptive responses are well understood. HSP90 prevents cellular damage by facilitating the refolding of misfolded proteins at high temperatures and removing heat-induced protein aggregates in metazoan species and yeast (Borkovich et al., 1989; Dickey et al., 2007). Accumulating

[1] Address correspondence to cmpark@snu.ac.kr.
The author responsible for distribution of materials integral to the findings presented in this article in accordance with the policy described in the Instructions for Authors (www.plantcell.org) is: Chung-Mo Park (cmpark@snu.ac.kr).
www.plantcell.org/cgi/doi/10.1105/tpc.17.00612

evidence also supports the notion that plant HSP90 proteins mediate various aspects of heat stress responses (Xu et al., 2012). It is notable that high-temperature stress influences virtually all facets of plant growth and development, from seed germination to flowering (Bita and Gerats, 2013). HSP90 also affects plant environmental performance and circadian clock function (Filichkin et al., 2015), implying that the interactions of HSP90 with distinct E3 ubiquitin ligases during plant environmental adaptation are more complicated than previously thought.

HSP90 acts as a molecular chaperone for the F-box protein ZEITLUPE (ZTL) in Arabidopsis (Kim et al., 2011). The ZTL E3 ubiquitin ligase acts as an evening-phased clock component that mediates proteasomal degradation of the circadian clock components TIMING OF CAB EXPRESSION1 (TOC1) and PSEUDO-RESPONSE REGULATOR5 (PRR5) (Más et al., 2003; Kiba et al., 2007). The levels of ZTL protein oscillate in a circadian manner. HSP90, in conjunction with GIGANTEA (GI), stabilizes ZTL in the afternoon (Kim et al., 2011). ZTL is unique among the known HSP90 clients in that the molecular chaperone stabilizes and facilitates the correct folding of this heat-denatured client (Cha et al., 2015). Together with the pivotal roles of HSP90 in thermal responses, these observations raise the possibility that the ZTL-HSP90 complex underlies the thermostable nature of the circadian clock in plants.

In this study, we demonstrated that ZTL, together with its interacting molecular chaperone HSP90, enhances thermotolerance during plant growth by promoting polyubiquitination of misfolded proteins at high temperatures. Whereas ZTL-HSP90 protein complexes were dispersed in the cytoplasm at normal temperatures, the protein complexes were associated with insoluble protein aggregates in the cytoplasm at high temperatures. Interestingly, circadian rhythms were more rapidly dampened in the ZTL-defective mutant compared with those in control plants under heat stress conditions. Together, we propose that the ZTL-mediated polyubiquitination of protein aggregates is essential for thermotolerance and provides the means for sustaining robust circadian clock function under stressful high-temperature conditions.

RESULTS

The *ztl-105* Mutant Exhibits Reduced Thermotolerance

Based on the finding that HSP90 mediates the stabilization of ZTL proteins (Kim et al., 2011; Cha et al., 2015, 2017), we hypothesized that ZTL is involved in the heat stress response. To examine this hypothesis, we first examined the thermosensitivity of ZTL-defective mutant and *ZTL*-overexpressing plants (Supplemental Figure 1). As ZTL protein abundance is under diurnal control (Kim et al., 2003), plants were treated with high temperatures at a specific time, the midpoint of the day under long days. We found that the *ztl-105* mutant exhibited significantly reduced thermotolerance, while *ZTL*-overexpressing plants exhibited enhanced thermotolerance compared with Col-0 plants (Figures 1A and 1B). Consistent with the altered thermal responses, chlorophyll contents were lower in the *ztl-105* mutant but higher in the *ZTL*-overexpressing plants (Figure 1C), supporting the notion that ZTL is involved in plant thermotolerance.

To investigate whether thermal responses vary over the day, we performed thermotolerance assays at different time points. At the end of the day, the reduced thermotolerance of *ztl-105* was still evident (Supplemental Figure 2). In contrast, at the end of the night, there were no significant differences in thermotolerance between Col-0 and *ztl-105* plants, indicating that ZTL-mediated thermal responses fluctuate throughout the diurnal cycle.

To verify that the reduced thermotolerance of *ztl-105* is caused by the loss-of-function mutation, the mutant was complemented with a genomic *ZTL* gene, whose expression was driven by the endogenous gene promoter. The reduced thermotolerance of *ztl-105* was successfully rescued in the complemented plants (Supplemental Figure 3), indicating that ZTL is functionally associated with the thermoresponsive phenotype of the mutant.

The *ztl-105* mutant exhibits a longer circadian period than Col-0 plants (Martin-Tryon et al., 2007). The question remained whether the thermal response of the mutant is associated with its longer circadian period. We examined the thermal responsiveness of another mutant with a long circadian period, *prr7-11* (Farré et al., 2005). The basal thermotolerance of *prr7-11* was not discernibly different from that of Col-0 plants (Supplemental Figure 4), unlike *ztl-105*, indicating that the reduced thermotolerance phenotype of *ztl-105* is independent of circadian periodicity.

We next examined whether ZTL is associated with heat acclimation. Plants were pretreated at 37°C before exposure to higher temperatures. Measurements of survival rates and chlorophyll contents revealed that acquired thermotolerance was reduced in *ztl-105* but enhanced in *ZTL*-overexpressing plants (Figures 1D to 1F and 1G to 1I, respectively), indicating that ZTL is associated with both basal and acquired thermotolerance responses.

Polyubiquitination Is Suppressed in the *ztl-105* Mutant under Heat Stress

A large set of HSPs and heat shock factors (HSFs) mediate heat stress response and signaling in Arabidopsis (von Koskull-Döring et al., 2007). We investigated whether ZTL-mediated thermotolerance is functionally linked with known HSPs and HSFs. Measurements of transcript level by RT-qPCR showed that the relative transcript levels of *HSP* and *HSF* were similar in Col-0 and *ztl-105* plants at high temperatures (Figure 2A). The dehydration-responsive element binding (DREB) transcription factors play a regulatory role in drought and heat stress responses (Lata and Prasad, 2011). Ascorbate peroxidase (APX) is an antioxidant enzyme that functions in a broad spectrum of abiotic stress responses, including heat stress, by detoxifying hydrogen peroxide (Panchuk et al., 2002). We found that the expression of *DREB* and *APX* was also unaffected by the *ztl-105* mutation (Figure 2B). These observations indicate that ZTL-mediated thermotolerance occurs independently of known heat stress signaling pathways, at least at the transcriptional level.

Under heat stress, misfolded proteins that are excluded from the refolding process undergo polyubiquitination and are subsequently degraded through the ubiquitin-proteasome pathways to maintain protein homeostasis (McClellan et al., 2005; Finka and Goloubinoff, 2013). We found that *ztl-105* is susceptible to high temperatures. Therefore, we investigated whether the ZTL enzyme mediates the heat-induced polyubiquitination process.

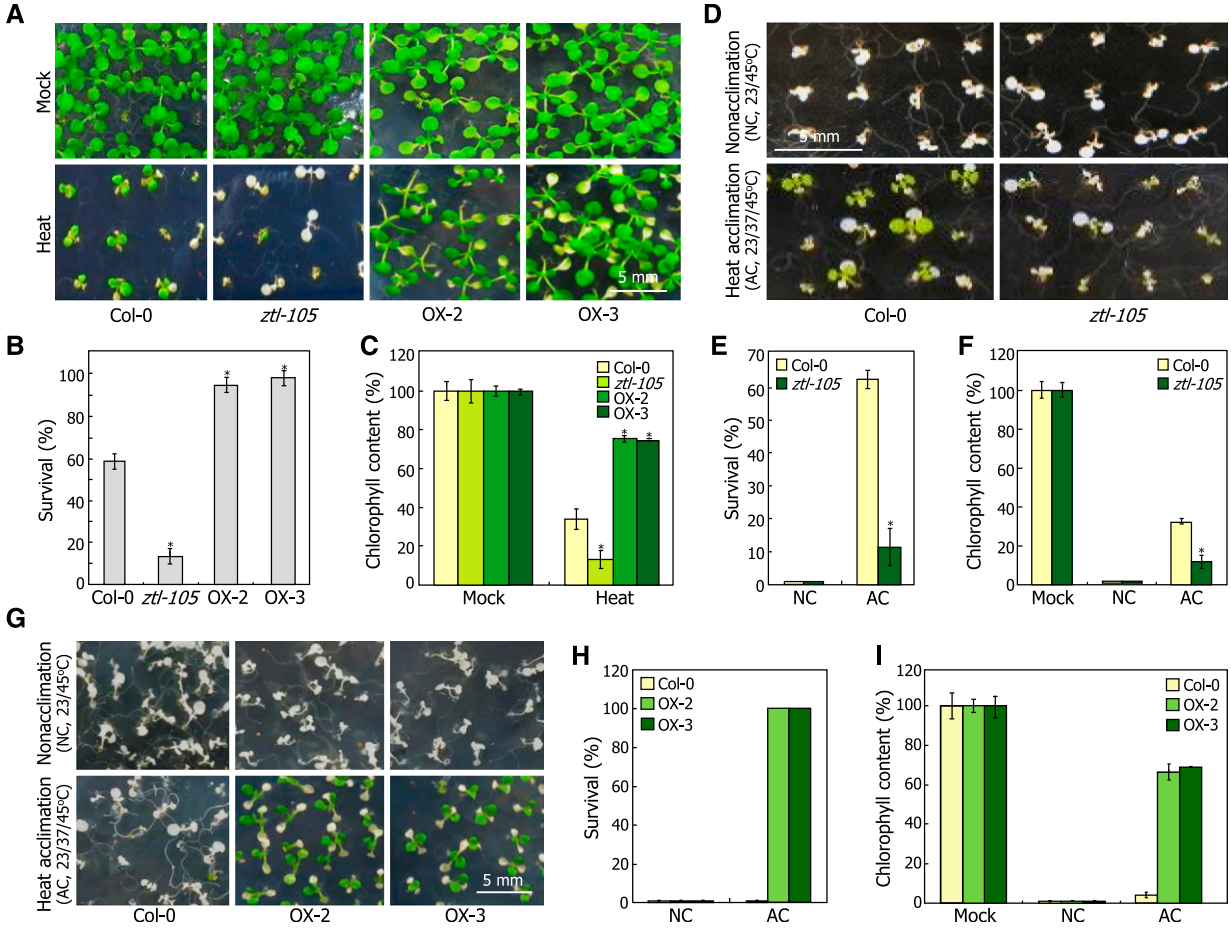

Figure 1. ZTL Is Functionally Associated with Thermotolerance.

(A) to **(C)** Reduced basal thermotolerance in *ztl-105*. One-week-old plants grown on MS-agar plates were exposed to 40°C at the midpoint of the day for 4.5 h in darkness and allowed to recover at 23°C for 5 d **(A)**. Two measurements of survival rates **(B)** and chlorophyll contents **(C)**, each consisting of 30 plants, were averaged and statistically analyzed (*t* test, *P < 0.01). Bars indicate SE of the mean. Transgenic plants (OX-2 and OX-3) in which the ZTL-coding sequence was overexpressed driven by the CaMV 35S promoter were included in the assays.

(D) to **(F)** Reduced acquired thermotolerance in *ztl-105*. One-week-old plants grown on MS-agar plates were preincubated at 37°C for 1 h in darkness and subsequently at 23°C for 2 h before exposure to 45°C for 1.5 h in darkness. The heat-treated plants were allowed to recover at 23°C for 5 d **(D)**. Survival rates **(E)** and chlorophyll contents **(F)** were measured as described above. NC, nonacclimation; AC, heat acclimation.

(G) to **(I)** Enhanced acquired thermotolerance in *ZTL*-overexpressing plants. One-week-old plants grown on MS-agar plates were preincubated at 37°C for 1 h in darkness and subsequently at 23°C for 2 h before exposure to 45°C for 3 h in darkness. The heat-treated plants were allowed to recover at 23°C for 5 d **(G)**. Two measurements of survival rates **(H)** and chlorophyll contents **(I)** were obtained, as described above.

Plants were exposed to 40°C, and polyubiquitinated proteins were immunologically detected in total protein extracts. Polyubiquitination was not altered in either Col-0 or *ztl-105* plants at 23°C in darkness (Figure 2C). Notably, following exposure to heat stress, the polyubiquitination level rapidly increased within one hour in Col-0 plants (Figure 2D). However, the rate of increase was notably reduced in the *ztl-105* mutant. In addition, the differential effects of heat stress on polyubiquitination were also observed in light-treated plants (Figure 2E), indicating that ZTL helps increase heat-induced polyubiquitination regardless of light conditions. Meanwhile, the reduced polyubiquitination was recovered in the *ztl-105* complemented lines (Supplemental Figure 5), further supporting the role of ZTL in heat-induced polyubiquitination.

Protein Aggregate Formation Increases in the *ztl-105* Mutant under Heat Stress

Misfolded proteins that form under unfavorable stress conditions are either refolded into their native conformations or deposited as insoluble aggregates, which are subsequently removed by the ubiquitin-proteasome pathways (McClellan et al., 2005; Finka and Goloubinoff, 2013). As a result, a reduction in polyubiquitination often accompanies the accumulation of insoluble aggregates. We found that ZTL enhances protein polyubiquitination under heat stress, suggesting that protein aggregates accumulate in *ztl-105*.

Total proteins were extracted from plants exposed to 40°C in darkness and fractionated into soluble and insoluble forms. We

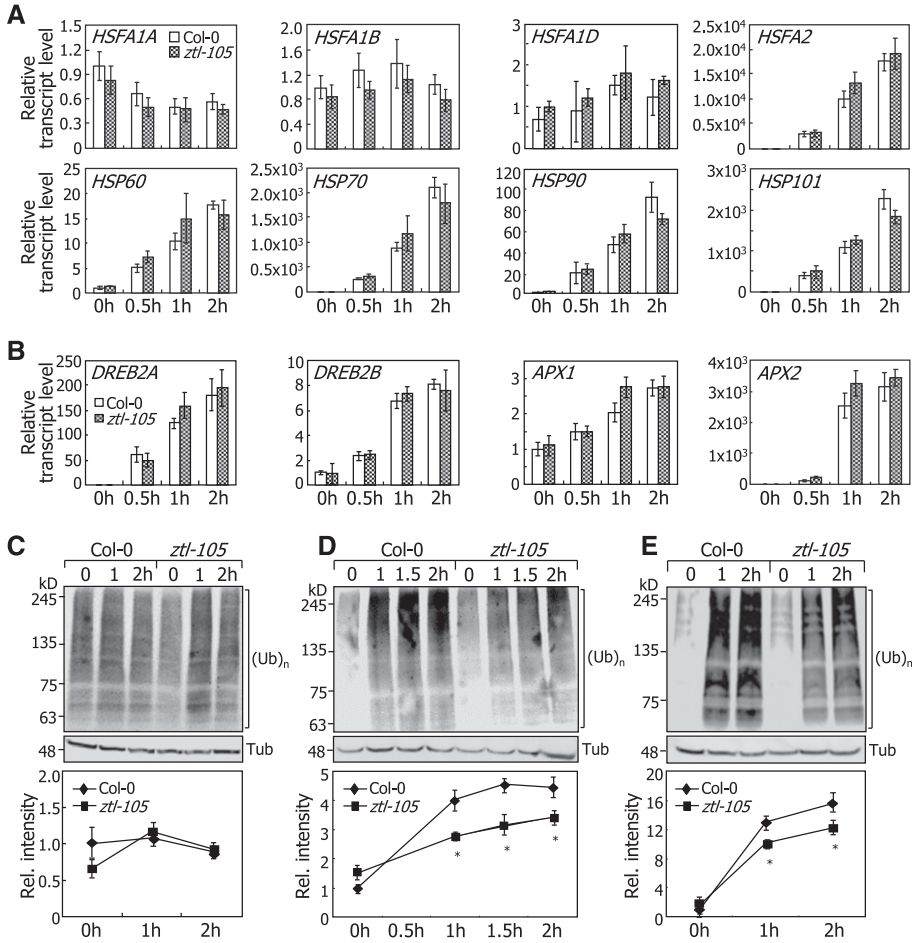

Figure 2. Heat-Induced Polyubiquitination Is Reduced in *ztl-105*.

(A) and **(B)** Quantification of the transcript levels of heat stress genes in *ztl-105*. Ten-day-old plants grown on MS-agar plates were exposed to 40°C at the midpoint of the day for the indicated time durations before harvesting whole plants for total RNA extraction. Transcript levels of *HSF* and *HSP* **(A)** and *DREB* and *APX* **(B)** were examined by RT-qPCR. Experiments were repeated three times, and the values were averaged (*t* test, $P < 0.01$). Bars indicate SE of the mean. Note that there are no significant differences in the transcript levels of the tested genes.

(C) to **(E)** Levels of polyubiquitinated proteins in heat-treated *ztl-105*. Eight-day-old plants grown on MS-agar plates were transferred to MS liquid culture at 23°C for 1 d, followed by exposure to either 23°C **(C)** or 40°C **(D)** in darkness for the indicated time durations. The plants were also exposed to 40°C in the light **(E)**. Total proteins were extracted from whole plants, and polyubiquitinated proteins $(Ub)_n$ were detected immunologically using an antiubiquitin (Ub) antibody. Tubulin (Tub) protein was also immunologically detected as a loading control. For each treatment, protein levels in three blots were quantified using ImageJ software (http://rsb.info.nih.gov/ij/) and averaged (*t* test, $^*P < 0.01$). Bars indicate SD.

found that the levels of insoluble protein aggregates were higher in the heat-treated *ztl-105* mutant versus Col-0 (Figure 3A), which is certainly related to the reduced polyubiquitination in the mutant at high temperatures (Figures 2D, 2E, and 3B). In contrast, the levels of insoluble protein aggregates decreased, but protein polyubiquitination increased, in *ZTL*-overexpressing plants compared with the wild type (Figures 3C and 3D), indicating that ZTL is important for clearing protein aggregates.

The molecular chaperone HSP90 is an interacting partner of ZTL (Kim et al., 2011) that mediates the polyubiquitination of cellular proteins at high temperatures. Notably, whereas most HSP90 protein was present in the soluble fraction under normal temperature conditions, it was detected in both the soluble and insoluble fractions at high temperatures (Figure 3A). These observations support the notion that ZTL and its interacting partner HSP90 constitute part of a heat-inducible protein quality control system, which is able to clear insoluble protein aggregates through the ubiquitin-proteasome pathways.

The next question was how heat stress affects the function of ZTL in the quality control of cellular proteins. *ZTL* transcript levels increased only slightly at high temperatures (Figure 3E). The protein levels of ZTL were unaltered by heat stress (Figure 3F). Therefore, it is evident that heat stress does not affect ZTL function at the levels of gene transcription and protein production and stability.

The subcellular localization of ubiquitin ligases underlies the ubiquitin-dependent degradation of their target proteins (Huett et al., 2012; Heck et al., 2010). We therefore examined the dynamic association of ZTL with protein aggregates at high temperatures.

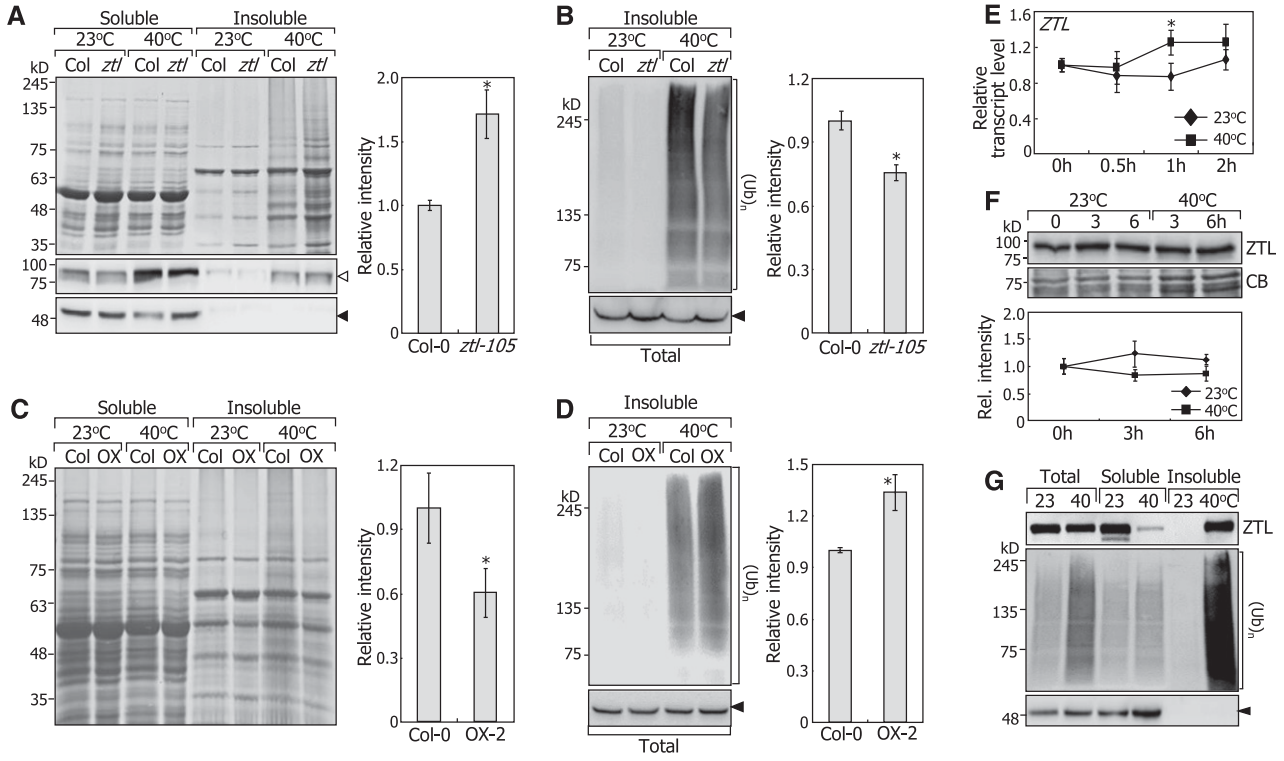

Figure 3. Insoluble Protein Aggregates Accumulate in *ztl-105* at High Temperatures.

(A) and **(B)** Levels of protein aggregates in *ztl-105*. Eight-day-old plants grown on MS-agar plates were transferred to MS liquid culture at 23°C for 1 d. At the midpoint of the day, the plants were exposed to 40°C in darkness for 2 h before preparing soluble and insoluble fractions. In **(A)**, protein blots were stained with Coomassie blue (uppermost panel), and HSP90 and Tub were immunologically detected (lower panels). Black and white arrowheads indicate HSP90 and Tub, respectively. Relative levels of accumulated aggregates at high temperatures were quantified using ImageJ software (right panel). Protein levels in three blots were averaged (*t* test, *P < 0.01). Bars indicate SD. In **(B)**, polyubiquitinated proteins [$(Ub)_n$] in insoluble fraction were immunologically detected. Protein levels in three blots were quantified as described in **(A)**.

(C) and **(D)** Levels of protein aggregates in *ZTL*-overexpressing OX-2 plants. In **(C)**, protein sample preparation, protein blots, and Coomassie blue staining were performed as described in **(A)**. Polyubiquitinated proteins $(Ub)_n$ in insoluble fraction were immunologically detected **(D)**.

(E) and **(F)** Effects of high temperatures on *ZTL* transcript abundance and ZTL protein stability. Ten-day-old plants grown on MS-agar plates were exposed to 40°C. Transcript levels were examined by RT-qPCR **(E)**. Biological triplicates were averaged (*t* test, *P < 0.01). Bars indicate SE of the mean. The $35S_{pro}$*:ZTL-MYC* transgenic plants were heat-treated and then ZTL-MYC proteins were immunologically detected **(F)**. CB, Coomassie blue-stained membrane.

(G) Enrichment of ZTL proteins in insoluble fraction. The $35S_{pro}$*:ZTL-MYC* transgenic plants were heat-treated as described in **(A)**, and protein fractions were prepared for the immunological detection of ZTL and $(Ub)_n$.

Transgenic plants overproducing ZTL fused with the MYC tag were heat-treated, and total proteins were separated into soluble and insoluble fractions. Interestingly, both ZTL proteins and polyubiquitinated proteins cofractionated in the insoluble fraction at 40°C (Figure 3G), indicating that ZTL proteins are shuttled to protein aggregates under heat stress, possibly in conjunction with HSP90.

To verify the role of ZTL in clearing insoluble aggregates at high temperatures, we employed nano-high-resolution liquid chromatography-tandem mass spectrometry (LC-MS/MS). Heat-induced insoluble protein bands were analyzed (Figure 4A), and several proteins that were predominant in *ztl-105* were identified (Figure 4B). We selected HEXOKINASE1 (HXK1) as a representative protein for kinetic accumulation assays of insoluble aggregates. As expected, HXK1 levels increased in the *ztl-105* insoluble fraction at high temperatures (Figure 4C), indicating that ZTL plays a role in clearing heat-induced protein aggregates.

ZTL interacts with HSP90 under normal conditions (Kim et al., 2011). HSP90 protein levels increase after exposure to heat stress (Meiri and Breiman, 2009). We observed that both ZTL and HSP90 proteins were enriched in insoluble aggregates at high temperatures. We therefore examined whether the ZTL-HSP90 interaction is affected under heat stress. Bimolecular fluorescence complementation (BiFC) assays, in which truncated yellow fluorescence protein fusions were transiently expressed in Arabidopsis protoplasts, revealed that the ZTL-HSP90 interaction still occurred at high temperatures (Figure 5A; Supplemental Figure 6). Notably, coimmunoprecipitation assays showed that the ZTL-HSP90 interaction increased after heat shock (Figure 5B), indicating that high temperatures increase the formation of ZTL-HSP90 protein complexes.

To more systematically examine the effects of high temperatures on the ZTL-HSP90 interaction, we performed additional coimmunoprecipitation assays by adjusting the amounts of

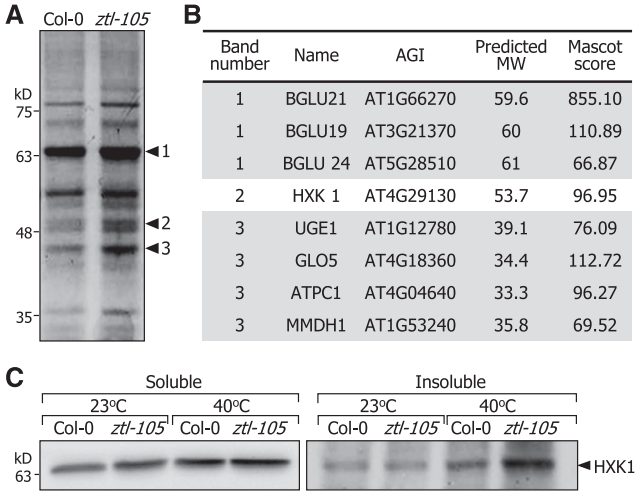

Figure 4. Nano-High-Resolution LC-MS/MS Spectrometry Analysis of Protein Aggregates at High Temperatures.

(A) Levels of protein aggregates at high temperatures. Eight-day-old plants grown on MS-agar plates were transferred to MS liquid culture at 23°C for 1 d, followed by exposure to 40°C in darkness for 2 h prior to the preparation of insoluble fraction. The protein gels were stained with Coomassie blue.
(B) List of proteins identified by nano-LC-MS/MS. Proteins were extracted from selected protein bands (labeled 1–3 in **[A]**). The extracted proteins were subjected to nano-high-resolution LC-MS/MS. Some of the proteins that were predominant in the protein aggregates of *ztl-105* samples, including HXK1, are listed.
(C) Increased HXK1 protein levels in insoluble aggregates from *ztl-105*. Soluble and insoluble protein fractions were prepared from heat-treated plants, as described above. HXK1 protein levels were examined immunologically using an anti-HXK1 antibody.

interacting proteins. Since HSP90 protein levels increased by approximately 4-fold under heat stress (Supplemental Figure 7A), the heat-treated samples were diluted four times so that the level of HSP90 proteins was equal to that in mock samples (Supplemental Figure 7B). The assays revealed that while the level of ZTL proteins was diluted in the heat-treated samples, the ZTL-HSP90 interaction occurred at a similar level in mock and heat-treated samples. Together, these observations indicate that the increased interaction between ZTL and HSP90 at high temperatures is directed not only by increased HSP90 protein abundance but also in part by the increased formation of ZTL-HSP90 protein complexes.

We further investigated the link between HSP90 with ZTL in heat-induced polyubiquitination using HSP90 RNAi plants, in which cytosolic HSP90 proteins are markedly depleted (Kim et al., 2011). Heat-induced polyubiquitination was markedly reduced in the HSP90 RNAi plants (Figure 5C), further supporting the functional linkage between ZTL and HSP90 in thermoinducible protein quality control.

The Circadian Clock Is Hypersensitive to High Temperatures in *ztl-105*

Our data indicate that ZTL is involved a protein quality control system that functions at high temperatures. ZTL is thought to be involved in the temperature compensation of the circadian clock at warm temperatures (27°C) (Edwards et al., 2005), raising the possibility that the ZTL-mediated thermal response is functionally associated with clock function.

Analyses of the rhythmic expression patterns of genes encoding CHLOROPHYLL A/B BINDING PROTEIN2 (CAB2), CATALASE3 (CAT3), and carotenoid and COLD, CIRCADIAN RNA BINDING2 (CCR2) showed that at 23°C, *ztl-105* exhibited longer periods compared with Col-0 plants (Supplemental Figure 8), as reported previously (Martin-Tryon et al., 2007). We investigated circadian rhythms in the *ztl-105* mutant after exposure to high temperatures. At 28°C, a temperature that does not induce a heat stress response, the rhythmic expression patterns of *CAB2* remained unaffected but had reduced amplitudes in both Col-0 and *ztl-105* plants (Figure 6A). As acquired thermotolerance is compromised in *ztl-105* (Figure 1D), we also tested rhythmicity in seedlings moved from 23°C to 35°C. The step-up in temperature caused a dramatic shift in the phase of *CAB2* and *CAT3* in Col-0 plants between days 1 and 2 (Figure 6B; Supplemental Figures 8 to 10). The period between days 1 and 2 was almost 32 h, whereas the period between days 2 and 3 was close to 24 h in Col-0

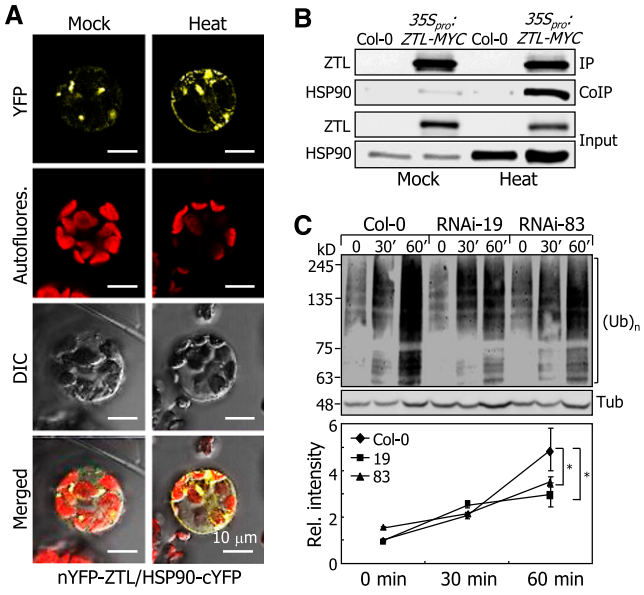

Figure 5. HSP90 Is Associated with Heat-Induced Polyubiquitination by Interacting with ZTL.

(A) BiFC investigating ZTL-HSP90 interactions. BiFC was employed to examine ZTL-HSP90 interactions in Arabidopsis protoplasts under mock (23°C) and heat treatment (1 h at 35°C) conditions.
(B) Coimmunoprecipitation. The *35S$_{pro}$:ZTL-MYC* transgenic plants were exposed to 40°C in darkness for 2 h. Immunoprecipitation (IP) was performed using magnetic beads, and the precipitates were used for the immunological detection of MYC-ZTL and HSP90. Input represents 5% of the IP reaction.
(C) Reduction in heat-induced polyubiquitination in HSP90 RNAi plants. Plants were grown and exposed to 40°C, as described in Figure 2D. Polyubiquitinated proteins were detected immunologically. Protein levels in three blots were quantified and averaged (*t* test, *P < 0.01). Bars indicate SE of the mean.

(Supplemental Figure 8C). This indicates that the shift to the higher temperature reset the phase of the clock, as observed in *Neurospora crassa* (Rensing et al., 1987). The rhythmic oscillations of transcript level in the *ztl-105* mutant showed a similar phase shift, as well as a much reduced amplitude (Figure 6B). These observations indicate that ZTL is required for robust circadian clock function under heat stress but is not related to temperature compensation of the clock. The rhythmic expression of *CAB2* was not detected in Col-0 or *ztl-105* plants at 42°C, when nonviability was observed (Figure 6C).

We found that HSP90 interacts with ZTL in modulating protein polyubiquitination at high temperatures (Figures 5A to 5C). Circadian rhythms were disturbed in *ztl-105* under identical conditions (Figure 6B). We therefore suspected that circadian rhythms would be altered in plants with reduced HSP90 activity. Consistent with the known roles of cytosolic HSP90 proteins in circadian clock function (Kim et al., 2011), circadian rhythms were largely disturbed in HSP90 RNAi plants at high temperatures (Figure 6D; Supplemental Figure 10), as observed in the *ztl-105* mutant. The rhythmic oscillations of transcript abundance of *TOC1* and *CAT3* also disappeared in the HSP90 RNAi plants at 35°C (Supplemental Figure 11).

We next investigated the link between the accumulation of protein aggregates and clock thermosensitivity by including MG132, a potent proteasome inhibitor (Lee and Goldberg, 1998), in the assays examining the circadian rhythmic expression of *CAB2*. At 23°C, the rhythmic expression of *CAB2* was evident in both Col-0 and *ztl-105* plants in the presence of MG132 (Figures 6E and 6F; Supplemental Figure 12). At 35°C, the circadian rhythms were still evident at ZT24-48 but disappeared in the presence of MG132 (Figure 6E). In contrast, the rhythmic expression pattern was not observed in *ztl-105*, even in the absence of MG132 (Figure 6F), demonstrating that ZTL plays a role in the thermostability of the clock by modulating the accumulation of protein aggregates.

ZTL modulates the protein stability of TOC1 and PRR5 through ubiquitin-mediated degradation pathways (Más et al., 2003; Kiba et al., 2007). We therefore investigated whether ZTL-mediated control of TOC1 and PRR5 protein stability is related to the disrupted circadian rhythms in the *ztl-105* mutant at high temperatures. While the protein levels of TOC1 and PRR5 were rapidly reduced during the dark period at 23°C (Figure 7A), such reductions were not observed at 35°C (Figure 7B), similar to the protein accumulation patterns in ZTL-defective mutants (Más et al., 2003; Kiba et al., 2007). In addition, TOC1 and PRR5 proteins

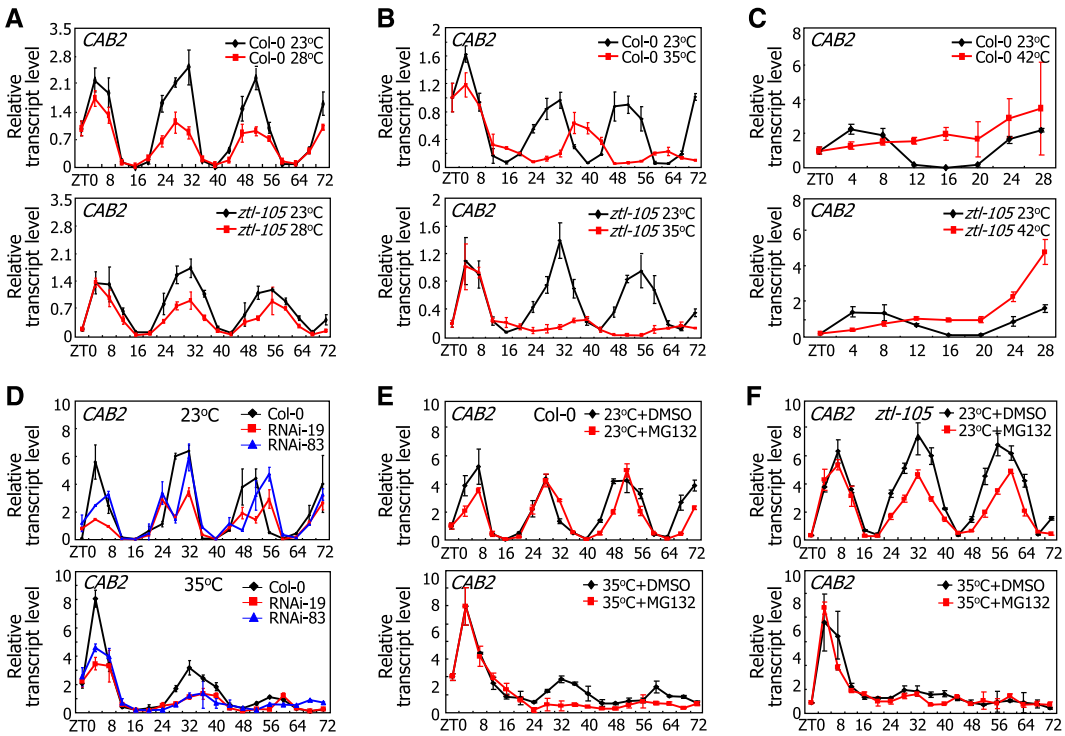

Figure 6. ZTL-Mediated Protein Quality Control Contributes to the Thermostability of the Clock.

Transcript levels were examined by RT-qPCR. Three measurements were repeated, and the values were averaged. Bars indicate SE of the mean.
(A) to **(C)** Disruption of circadian rhythms in *ztl-105* at high temperatures. Seven-day-old plants grown on MS-agar plates at 23°C were incubated at 28°C **(A)**, 35°C **(B)**, or 42°C **(C)** in the light. ZT, zeitgeber time.
(D) Disruption of circadian rhythms in HSP90 RNAi plants. Plant growth, heat treatments, and transcript level analysis were performed as described above.
(E) and **(F)** Effects of MG132 on circadian rhythms. Six-day-old plants grown on MS-agar plates at 23°C were transferred to MS liquid culture for 1 d. The plants were then transferred to MS liquid culture supplemented with 50 mM MG132 and incubated at either 23°C or 35°C in the light. Circadian rhythms were examined in Col-0 **(E)** and *ztl-105* plants **(F)**.

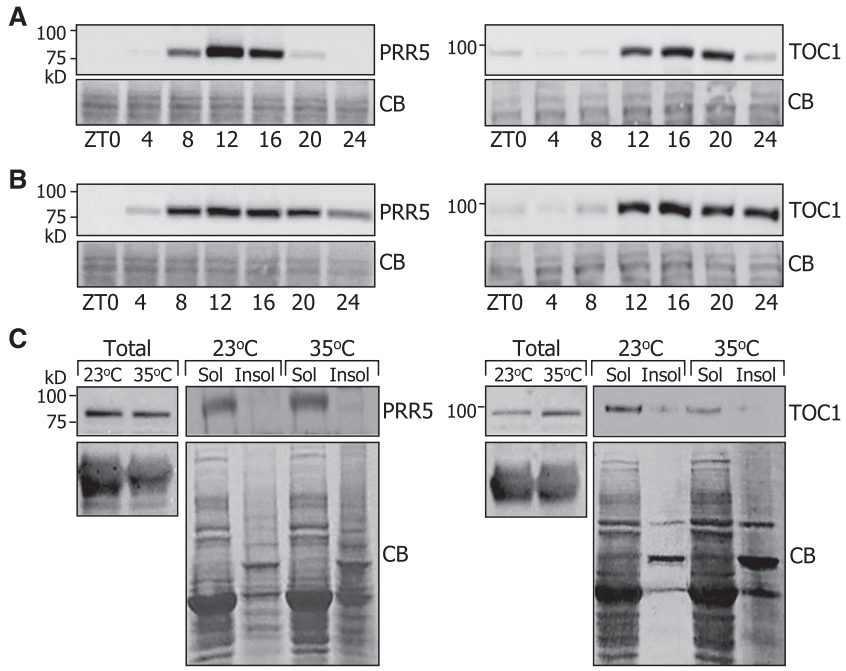

Figure 7. Diurnal Rhythmic Accumulation of PRR5 and TOC1 Is Disrupted at High Temperatures.

(A) and **(B)** Accumulation patterns of PRR5 and TOC1 proteins. The *PRR5*$_{pro}$*:PRR5-GFP* and *TOC1*$_{pro}$*:TOC1-YFP* transgenic plants in the Col-0 background were described previously (Más et al., 2003; Kiba et al., 2007). The plants were grown on MS-agar plates at 23°C for 9 d and either kept at 23°C or transferred to 35°C for 1 d (**[A]** and **[B]**, respectively). Whole plants were harvested at the indicated ZT points for total protein extraction. PRR5-GFP and TOC1-YFP proteins were immunologically detected using polyclonal anti-GFP antibody produced in rabbit (catalog no. ab6556; Abcam). CB, Coomassie blue-stained membrane.

(C) Subcellular localization of PRR5 and TOC1. The heat-treated transgenic plants described in **(A)** were used for the preparation of soluble and insoluble fractions. Cell fractionation was performed as described in Figure 3A in the presence of 50 mM MG132. PRR5-GFP and TOC1-YFP proteins were immunodetected as described above. Parts of CB (membranes) are displayed at the bottom as a loading control.

remained in the soluble fraction (Figure 7C), while ZTL proteins were fractionated into the insoluble fraction (Figure 3G). These observations indicate that TOC1 and PRR5 are not directly involved in ZTL-mediated stabilization of the clock function at high temperatures.

Altogether, we propose that the ZTL/HSP90-mediated protein quality control system confers sustainability of plant growth and, possibly, robust clock function under heat stress conditions (Figure 8). Upon exposure to stressful high temperature conditions, ZTL enhances the polyubiquitination of misfolded proteins to direct them toward the ubiquitin-proteasome pathways, thus eliminating the accumulation of protein aggregates that are toxic to cellular components. Our model provides a distinct molecular link between protein quality control and thermotolerance responses in plants.

DISCUSSION

ZTL and HSP90 Mediate a Thermoresponsive Protein Quality Control Mechanism

Protein misfolding is a common cellular event that occurs continuously as living organisms age or encounter environmental extremes, such as high temperatures and oxidative stress. Versatile protein quality control systems have evolved to cope with misfolded proteins and their insoluble aggregates by either facilitating refolding reactions or clearing insoluble aggregates (McClellan et al., 2005; Finka and Goloubinoff, 2013).

In plants, distinct ubiquitin-proteasome systems are responsible for the degradation of irreversibly aggregated proteins; the accompanying E3 ubiquitin ligase enzymes have been functionally characterized. The ubiquitin ligase CHIP polyubiquitinates misfolded proteins that are targeted for degradation to eliminate proteotoxicity under environmental stress conditions (Zhou et al., 2014; Lee et al., 2009; Samant et al., 2014). Meanwhile, the autophagy receptor NEXT TO BRCA1 GENE1 (NBR1) mediates the autophagosomal degradation of ubiquitinated protein aggregates (Zhou et al., 2013). CHIP and NBR1 mediate two distinct but mutually complementary anti-proteotoxic pathways that function in abiotic stress responses in plants (Zhou et al., 2014).

Molecular chaperones are a group of proteins that not only facilitate proper folding of newly synthesized polypeptides but also mediate controlled degradation of misfolded proteins and their aggregates by forming chaperone-E3 ubiquitin ligase complexes (McClellan et al., 2005; Finka and Goloubinoff, 2013). Many molecular chaperones identified thus far are HSPs, which are produced in response to elevated temperatures in plants

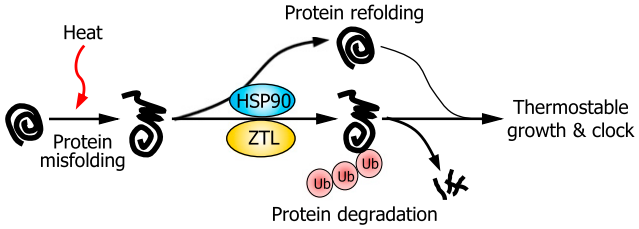

Figure 8. Working Model for the ZTL-Mediated Thermostabilization of Growth and Circadian Clock Function.

Under heat stress conditions, ZTL forms a complex with HSP90 that eliminates insoluble protein aggregates via polyubiquitination-mediated protein degradation. Meanwhile, HSP90 facilitates the refolding of misfolded proteins to maintain protein homeostasis. Since protein aggregates are toxic to cell viability and the circadian clock, these protein quality control processes confer plants with increased resistance to high temperature stress.

(Zhou et al., 2014; Krishna and Gloor, 2001; Xu et al., 2012; Bita and Gerats, 2013). Among plant HSPs, HSP90 has been the most extensively studied for its roles in plant responses to environmental stresses, including defense mechanisms (Xu et al., 2012), phenotypic plasticity (Sangster and Queitsch, 2005), and buffering of genetic variations (Sangster et al., 2008). In particular, high temperatures trigger HSP90 production, which plays a role in the assembly and maintenance of the 26S proteasome (Imai et al., 2003), suggesting HSP90 plays versatile roles in shaping protein turnover under stressful environments.

HSP90 plays a central role in maintaining animal circadian systems (Schneider et al., 2014). In plants, a well-known substrate of HSP90 is the F-box-containing ZTL ubiquitin ligase, which functions in the circadian clock (Kim et al., 2011). HSP90 stabilizes ZTL, and HSP90-mediated maturation of ZTL is essential for clock function (Kim et al., 2011). The HSP90-mediated stabilization of ZTL also contributes to the rhythmic accumulation of tetrapyrroles in chloroplasts, which in turn regulates the oscillated expression of genes encoding C-REPEAT BINDING FACTOR transcription factors (Norén et al., 2016). These observations support a potential role for the ZTL-HSP90 module in the intersection between the circadian clock and plastid signaling pathways.

In this study, we demonstrated that ZTL and HSP90 constitute part of the ubiquitin-proteasome-dependent protein quality control mechanism, which enhances the thermotolerance of plant growth and maintains thermostability of circadian clock function. In the ZTL-defective *ztl-105* mutant, protein polyubiquitination was reduced, but insoluble protein aggregates accumulated. We also found that ZTL and HSP90 were cofractionated with insoluble aggregates under heat stress, indicating that the ZTL-HSP90-mediated protein quality control system plays a major role in the degradation of irreversibly misfolded proteins that accumulate under heat stress. While the ZTL-HSP90 pathway thermostabilizes the clock function, it is not involved in the temperature compensation of the clock.

The CHIP-defective mutants are thermosusceptible, and insoluble protein aggregates accumulate in these mutants (Samant et al., 2014). Notably, polyubiquitination levels are also higher in the mutants than wild type, which is in contrast to the reduced polyubiquitination in *ztl-105* (this work) and in yeast mutants lacking various ubiquitin ligase enzymes (Fang et al., 2011; Yoo et al., 2015). This distinction suggests that the CHIP-mediated quality control mechanism is somewhat distinct from those mediated by other E3 enzymes to maintain protein homeostasis.

ZTL Sustains the Thermostability of the Circadian Clock

It is currently unclear how the ZTL/HSP90 system confers enhanced high-temperature tolerance to the clock function. One possibility is that clock components or those mediating clock input and output signals are misfolded upon exposure to high temperatures, forming insoluble aggregates that disrupt protein homeostasis of the clock function. Under this scenario, ZTL would provide a finely tuned protein turnover mechanism targeting heat-induced aggregates of the clock components. Alternatively, the accumulation of denatured or damaged cellular proteins could provoke cytotoxicity, resulting in an overall dysfunction of cellular activities, including the clock function. We found that thermotolerance is reduced and circadian rhythms are disturbed in *ztl-105* at high temperatures, supporting the latter possibility.

Previous and current data support the notion that ZTL modulates the clock function under both normal and stressful conditions. The ZTL enzyme degrades TOC1 and PRR5 in a circadian rhythmic pattern (Más et al., 2003; Kiba et al., 2007). We found that HSP90 and ZTL accumulate in insoluble protein aggregates under heat stress. One plausible explanation is that ZTL plays dual roles in maintaining the clock function. Under normal temperature conditions, it directs the dark-dependent degradation of TOC1 and PRR5 via the ubiquitin-proteasome pathway (Más et al., 2003; Kiba et al., 2007). On the other hand, when plants are exposed to high temperatures, ZTL and HSPs constitute part of the proteasomal protein quality control machinery that eliminates insoluble protein aggregates that inevitably form under this stressful condition. TOC1 and PRR5 remained soluble at high temperatures and were not targeted by the ZTL-HSP90 module, suggesting that ZTL mediates clock thermostability by targeting cellular proteins other than TOC1 and PRR5. The ZTL-mediated protein quality control system may also function under other stress conditions, such as oxidative stress and high salinity, which profoundly influence clock function (Marcolino-Gomes et al., 2014; Tamaru et al., 2013).

More work is required to elucidate the molecular mechanism that underlies the functions of ZTL and HSP90 in the heat-responsive protein quality control system. Based on their roles in plant thermotolerance and clock thermostability, the ZTL-HSP90 pathway would require additional cochaperones, such as HSP70 or GI. GI forms a ternary complex with HSP90 and ZTL, which functions in the maturation process of ZTL to maintain the clock function under normal temperature conditions (Cha et al., 2017). It is likely that GI also contributes to the thermotolerance response and clock thermostability by facilitating ZTL folding.

METHODS

Plant Materials and Growth Conditions

All *Arabidopsis thaliana* lines used in this study were in the Columbia (Col-0) background. Sterilized seeds were stratified at 4°C in darkness for 3 d and allowed to germinate on 0.5× Murashige and Skoog-agar plates (hereafter referred to as MS-agar plates) at 23°C under long days (LDs; 16 h light and

8 h dark). White light illumination (120 μmol photons m^{-2} s^{-1}) was provided by fluorescent FLR40D/A tubes (Osram).

The T-DNA insertional knockout mutants *prr7-11* and *ztl-105* were described previously (Yamamoto et al., 2003; Martin-Tryon et al., 2007). The MYC-coding sequence was fused in-frame to the 3′ end of the ZTL-coding sequence, and the gene fusion was subcloned into the binary pBA002 vector under the control of either the CaMV 35S promoter or the endogenous *ZTL* promoter, consisting of an ?1.8-kb sequence region upstream of the translational start site (Baudry et al., 2010). The expression constructs were transformed into Col-0 or *ztl-105* plants (Clough and Bent, 1998), resulting in $35S_{pro}$*:ZTL-MYC* or ZTL_{pro}*:ZTL-MYC ztl-105*, respectively. The ZTL-coding sequence was also subcloned into the binary pB2GW7 vector under the control of the CaMV 35S promoter, and the expression construct was transformed into Col-0 plants. The *ZTL*-overexpressing plants were used in thermotolerance assays.

Transcript Level Measurement

Total RNA samples were extracted from 10-d-old seedlings grown on MS-agar plates and pretreated with RNase-free DNase to eliminate genomic DNA contamination before RT-qPCR. RT-qPCR was performed in 96-well blocks with an Applied Biosystems 7500 real-time PCR system using SYBR Green I master mix in a volume of 20 μL. PCR primers were designed using Primer Express Software installed in the system; the primers are listed in Supplemental Table 1. Individual PCR reactions were set up as follows: 10 min at 95°C, followed by 35 to 40 cycles of 15 s at 95°C for denaturation and 1 min at 60°C for annealing and polymerization and an additional round of 1 min at 65°C at the end of the thermal cycles for the completion of PCR. The *eIF4A* gene (At3g13920) was included in the reactions as an internal control to normalize the variations in the amounts of cDNA used (Gutierrez et al., 2008).

All RT-qPCR was performed using three independent samples prepared from different plants grown under identical conditions. The comparative $\Delta\Delta C_T$ method was employed to evaluate relative quantities of individual amplified products in the samples. The threshold cycle C_T was automatically determined for each reaction using default parameters. The specificity of RT-qPCR was determined by melt curve analysis of the amplified products using the standard method installed in the system.

Thermotolerance Assay

The assays were performed essentially as described previously (Yoo et al., 2006), but with some modifications. Seven-day-old seedlings grown on MS-agar plates were exposed to 40°C for 4.5 h in darkness and allowed to recover at 23°C for 5 d under LDs. Survival of heat-treated seedlings was decided based on the presence of newly developing leaves. For the heat acclimation assays, seedlings were exposed to 37°C for 1 h and incubated at 23°C for 2 h before exposure to 45°C for 1.5 h in darkness. The heat-treated seedlings were then allowed to recover at 23°C for 5 d under LDs.

Chlorophyll Contents Measurements

Measurements of chlorophyll contents were performed as described previously (Lee et al., 2012). Briefly, plant materials were ground in liquid nitrogen, and chlorophylls were extracted with *N*,*N*-dimethylformamide. The extract was incubated at 4°C for 1 h in complete darkness. Chlorophyll contents were assayed by measuring absorbance at 652, 665, and 750 nm using a diode array spectrophotometer (WPA Biowave).

Detection of Polyubiquitinated Proteins

Eight-day-old seedlings grown on MS-agar plates were transferred to MS liquid culture for 1 d under LDs before exposure to 40°C. Plant materials were ground in liquid nitrogen, and total proteins were eluted with 2× SDS-PAGE loading buffer (100 mM Tris-Cl, pH 6.8, 4% SDS, 0.2% bromophenol blue, 20% glycerol, and 200 mM DTT) and boiled for 10 min. The boiled extract was clarified by centrifugation at 23°C for 10 min at 12,000*g*. Fifteen microliters of the supernatant was subjected to 6% SDS-PAGE and transferred onto a PVDF membrane (catalog no. IPVH00010; Millipore). Polyubiquitinated proteins were detected immunologically using a monoclonal antiubiquitin antibody produced in mouse (catalog no. sc-8017; Santa Cruz Biotechnology; diluted to 1:1000). For the secondary antibody, a goat anti-mouse IgG-horseradish peroxidase (HRP) (catalog no. sc-2005; Santa Cruz Biotechnology; diluted to 1:5000) was used. After incubation with the secondary antibody, HRP-conjugated proteins were visualized using the West Save Up system (catalog no. LF-QC0101; Abfrontier). The relative intensities of polyubiquitinated proteins were quantified using ImageJ software (https://imagej.nih.gov/ij/).

Fractionation of Soluble and Insoluble Proteins

Protein fractionation was performed as described previously (Coll et al., 2014). Plant materials were ground in liquid nitrogen and suspended in buffer B containing apyrase (catalog no. A6535; Sigma-Aldrich) and/or MG132. The protein extract was passed through a cell strainer with a pore sizes of 70 μm (Fisher Scientific), and the solution was centrifuged sequentially at 2000*g* at 10 min, followed by centrifugation at 3000*g* for 10 min at 4°C. The supernatant was centrifuged again at 16,000*g* at 4°C for 90 min. The supernatant and the pellet correspond to the soluble and insoluble fractions, respectively. The pellet was washed three times with fresh buffer B supplemented with 2% Nonidet P-40, each by centrifugation at 16,000*g* for 30 min. The pellet was resuspended in fresh buffer B and sonicated using an ultrasonic cleaner (SaeHan ultrasonic). The solutions were mixed with 5× SDS-PAGE loading buffer and boiled for 10 min.

The samples were analyzed on 6% and 10% SDS-PAGE gels. The 6% gel was either Coomassie blue-stained or subjected to immunoblotting analysis using an antiubiquitin antibody (Santa Cruz Biotechnology). A modified version of Coomassie blue staining was employed to detect the fractionated proteins with improved sensitivity (Wang et al., 2007). The 10% gel was blotted onto PVDF membrane, and HSP90.1, tubulin, and ZTL-MYC proteins were detected immunologically using a polyclonal anti-HSP90.1 antibody produced in rabbit (catalog no. AS08 346; Agrisera; diluted to 1:1000), a monoclonal anti-tubulin antibody produced in mouse (catalog no. T9026; Sigma-Aldrich; diluted to 1:500), and a monoclonal anti-MYC antibody produced in mouse (catalog no. 05-724; Millipore; diluted to 1:1000), respectively. For the secondary antibodies, a goat anti-mouse IgG-HRP (Santa Cruz Biotechnology) and a goat anti-rabbit IgG-HRP (catalog no. sc-2030; Santa Cruz Biotechnology; diluted to 1:5000) antibody were used.

Mass spectrometry of insoluble proteins was performed at the National Instrumentation Center for Environmental Management, Seoul National University, using a nano-high-resolution LC-MS/MS spectrometer (Thermo Scientific). Among the identified proteins, HXK1 proteins were immunologically detected using a polyclonal anti-HXK1 antibody produced in rabbit (catalog no. AS12 2601; Agrisera; diluted to 1:1000).

Protein Stability Assay

To examine the stability of ZTL proteins at high temperatures, $35S_{pro}$*:ZTL-MYC* transgenic plants were grown on MS-agar plates for 10 d under LDs. After incubation at 40°C in darkness, whole plants were harvested for total protein extraction. ZTL proteins were detected immunologically using an anti-MYC antibody (Millipore).

BiFC Assay

The assays were conducted as described previously (Seo et al., 2012). Full-size ZTL- and HSP90.1-coding sequences were fused in-frame to the 3′ end of a gene sequence encoding the N-terminal half of enhanced YFP in the pSATN-nEYFP-C1 vector (E3081) or to the 3′ end of a gene sequence encoding the C-terminal half of enhanced YFP in the pSATN-cEYFP-C1 vector (E3082). The expression constructs were cotransformed into Arabidopsis mesophyll protoplasts by the PEG-calcium transfection method (Yoo et al., 2007). Transformed protoplasts were incubated for 16 h under constant light, and reconstitution of YFP fluorescence was monitored by fluorescence microscopy under a Zeiss LSM510 confocal microscope (Carl Zeiss) with the following filter setup: 514 nm for excitation, 535 to 590 nm for YFP, and 690 to 730 nm for autofluorescence.

Coimmunoprecipitation Assays

Plants were grown on MS-agar plates for 9 d at 23°C. After incubation at 40°C in darkness for 2 h, whole plants were harvested for total protein extraction. Plant materials were ground in liquid nitrogen, and proteins were extracted in coimmunoprecipitation buffer (50 mM Tris-Cl, pH 7.4, 500 mM NaCl, 10% glycerol, 5 mM EDTA, 1% Triton X-100, and 1% Nonidet P-40) containing protease inhibitor cocktail tablets (catalog no. 11836153001; Sigma-Aldrich). Five percent of the extracts was used as the input control. The protein extracts were incubated with 20 μL polyclonal anti-c-Myc agarose affinity gel antibody produced in rabbit (catalog no. A7470; Sigma-Aldrich) for 1 h at 4°C. The beads were then washed five times with fresh coimmunoprecipitation buffer. To elute the proteins, 40 μL of 2× SDS loading buffer was added to the beads, followed by boiling for 10 min. Twenty percent of the eluted proteins were used as IP control. Anti-MYC (Millipore) and an anti-HSP90.1 (Agrisera) antibodies were used for the detection of ZTL-MYC and HSP90.1, respectively.

Circadian Rhythm Measurements

One-week-old plants grown on MS-agar plates under LDs were shifted from 23°C to 23°C, 28°C, 35°C, or 42°C for up to 3 d under constant light conditions at ZT0. Whole plant materials were harvested at the appropriate ZT points for total RNA extraction. Gene transcript levels were examined by RT-qPCR. The period and relative amplitude error of rhythmicity were calculated using BioDare2 software (https://biodare2.ed.ac.uk/welcome).

Accession Numbers

Sequence data from this article can be found in the Arabidopsis Genome Initiative databases under the following accession numbers: *eIF4A* (At3g13920), *DREB2A* (At5g05410), *DREB2B* (At3g11020), *APX1* (At1g07890), *APX2* (At3g09640), *HSFA1a* (At4g17750), *HSFA1b* (At5g16820), *HSFA1d* (At1g32330), *HSFA2* (At2g26150), *HSP60* (At3g23990), *HSP70* (At3g12580), *HSP90* (At5g52640), *HSP101* (At1g74310), *TOC1* (At5g61380), *PRR5* (At5g24470), *PRR7* (At5g02810), *CAT3* (At1g20620), *CCR2* (At1g06820), and *ZTL* (At5g57360).

Supplemental Data

Supplemental Figure 1. Molecular Validation of *ZTL*-Overexpressing Plants.

Supplemental Figure 2. Thermal Responses Depend on Diurnal Cycles.

Supplemental Figure 3. Complementation of the *ztl-105* Mutant.

Supplemental Figure 4. Thermal Responses Are Independent of Long Periodicity.

Supplemental Figure 5. Levels of Polyubiquitinated Proteins in *ztl-105* Complemented Lines.

Supplemental Figure 6. Bimolecular Fluorescence Complementation Assays of ZTL-HSP90 Interactions.

Supplemental Figure 7. Effects of High Temperatures on HSP90-ZTL Interactions.

Supplemental Figure 8. Disturbed Circadian Rhythms in *ztl-105* under Heat Stress Conditions.

Supplemental Figure 9. Transcript Levels of *TOC1* and *CAT3* under Heat Stress Conditions.

Supplemental Figure 10. Changes in Circadian Clock Rhythms in HSP90 RNAi Plants at High Temperatures.

Supplemental Figure 11. Transcript Levels of *TOC1* and *CAT3* under Heat Stress Conditions.

Supplemental Figure 12. Disruption of Circadian Clock Rhythms by MG132 Treatment.

Supplemental Table 1. Primers Used in RT-qPCR and Gene Cloning.

ACKNOWLEDGMENTS

We thank David Somers for providing the HSP90 RNAi lines. This work was supported by the National Research Foundation of Korea Leaping Research (NRF-2015R1A2A1A05001636) and Global Research Lab (NRF-2012K1A1A2055546) Programs and the Rural Development Administration of Korea Next-Generation BioGreen 21 Program (Plant Molecular Breeding Center No. PJ0111532015). K.-E.G. was partially supported by the Global PhD Fellowship Program through the National Research Foundation of Korea (NRF-2015H1A2A1034250). This work was supported in part by the TRE program at King Saud University.

AUTHOR CONTRIBUTIONS

C.-M.P. and K.-E.G. conceived the project and designed the experiments. C.-M.P prepared the manuscript with contributions from K.-E.G. K.-E.G. and H.-J.L. performed the experiments. C.-M.P., K.-E.G., and W.-Y.K. analyzed the data. M.F, Q.S., and A.A. provided scientific discussion on the ubiquitination data.

Received August 1, 2017; revised October 6, 2017; accepted October 20, 2017; published October 23, 2017.

REFERENCES

Baudry, A., Ito, S., Song, Y.H., Strait, A.A., Kiba, T., Lu, S., Henriques, R., Pruneda-Paz, J.L., Chua, N.H., Tobin, E.M., Kay, S.A., and Imaizumi, T. (2010). F-box proteins FKF1 and LKP2 act in concert with ZEITLUPE to control *Arabidopsis* clock progression. Plant Cell **22:** 606–622.

Bita, C.E., and Gerats, T. (2013). Plant tolerance to high temperature in a changing environment: scientific fundamentals and production of heat stress-tolerant crops. Front. Plant Sci. **4:** 273.

Borkovich, K.A., Farrelly, F.W., Finkelstein, D.B., Taulien, J., and Lindquist, S. (1989). hsp82 is an essential protein that is required in higher concentrations for growth of cells at higher temperatures. Mol. Cell. Biol. **9:** 3919–3930.

Cha, J.Y., Kim, M.R., Kim, W.Y., and Kim, M.G. (2015). Development of *in vitro* HSP90 foldase chaperone assay using a GST-fused real-substrate, ZTL (ZEITLUPE). J. Plant Biol. **58:** 236–241.

Cha, J.Y., Kim, J., Kim, Y.S., Zeng, Q., Wang, L., Lee, S.Y., Kim, W.Y., and Somers, D.E. (2017). GIGANTEA is a co-chaperone which facilitates maturation of ZEITLUPE in the Arabidopsis circadian clock. Nat. Commun. **8:** 3.

Clough, S.J., and Bent, A.F. (1998). Floral dip: a simplified method for *Agrobacterium*-mediated transformation of *Arabidopsis thaliana*. Plant J. **16:** 735–743.

Coll, N.S., Smidler, A., Puigvert, M., Popa, C., Valls, M., and Dangl, J.L. (2014). The plant metacaspase AtMC1 in pathogen-triggered programmed cell death and aging: functional linkage with autophagy. Cell Death Differ. **21:** 1399–1408.

Dickey, C.A., et al. (2007). The high-affinity HSP90-CHIP complex recognizes and selectively degrades phosphorylated tau client proteins. J. Clin. Invest. **117:** 648–658.

Edwards, K.D., Lynn, J.R., Gyula, P., Nagy, F., and Millar, A.J. (2005). Natural allelic variation in the temperature-compensation mechanisms of the *Arabidopsis thaliana* circadian clock. Genetics **170:** 387–400.

Fang, N.N., Ng, A.H., Measday, V., and Mayor, T. (2011). Hul5 HECT ubiquitin ligase plays a major role in the ubiquitylation and turnover of cytosolic misfolded proteins. Nat. Cell Biol. **13:** 1344–1352.

Farré, E.M., Harmer, S.L., Harmon, F.G., Yanovsky, M.J., and Kay, S.A. (2005). Overlapping and distinct roles of PRR7 and PRR9 in the *Arabidopsis* circadian clock. Curr. Biol. **15:** 47–54.

Filichkin, S.A., Cumbie, J.S., Dharmawardhana, P., Jaiswal, P., Chang, J.H., Palusa, S.G., Reddy, A.S., Megraw, M., and Mockler, T.C. (2015). Environmental stresses modulate abundance and timing of alternatively spliced circadian transcripts in *Arabidopsis*. Mol. Plant **8:** 207–227.

Finka, A., and Goloubinoff, P. (2013). Proteomic data from human cell cultures refine mechanisms of chaperone-mediated protein homeostasis. Cell Stress Chaperones **18:** 591–605.

Finka, A., Sood, V., Quadroni, M., Rios, Pde.L., and Goloubinoff, P. (2015). Quantitative proteomics of heat-treated human cells show an across-the-board mild depletion of housekeeping proteins to massively accumulate few HSPs. Cell Stress Chaperones **20:** 605–620.

Gutierrez, L., Mauriat, M., Guénin, S., Pelloux, J., Lefebvre, J.F., Louvet, R., Rusterucci, C., Moritz, T., Guerineau, F., Bellini, C., and Van Wuytswinkel, O. (2008). The lack of a systematic validation of reference genes: a serious pitfall undervalued in reverse transcription-polymerase chain reaction (RT-PCR) analysis in plants. Plant Biotechnol. J. **6:** 609–618.

Heck, J.W., Cheung, S.K., and Hampton, R.Y. (2010). Cytoplasmic protein quality control degradation mediated by parallel actions of the E3 ubiquitin ligases Ubr1 and San1. Proc. Natl. Acad. Sci. USA **107:** 1106–1111.

Huett, A., Heath, R.J., Begun, J., Sassi, S.O., Baxt, L.A., Vyas, J.M., Goldberg, M.B., and Xavier, R.J. (2012). The LRR and RING domain protein LRSAM1 is an E3 ligase crucial for ubiquitin-dependent autophagy of intracellular *Salmonella typhimurium*. Cell Host Microbe **12:** 778–790.

Imai, J., Maruya, M., Yashiroda, H., Yahara, I., and Tanaka, K. (2003). The molecular chaperone Hsp90 plays a role in the assembly and maintenance of the 26S proteasome. EMBO J. **22:** 3557–3567.

Kiba, T., Henriques, R., Sakakibara, H., and Chua, N.H. (2007). Targeted degradation of PSEUDO-RESPONSE REGULATOR5 by an SCF^{ZTL} complex regulates clock function and photomorphogenesis in *Arabidopsis thaliana.* Plant Cell **19:** 2516–2530.

Kim, T.S., Kim, W.Y., Fujiwara, S., Kim, J., Cha, J.Y., Park, J.H., Lee, S.Y., and Somers, D.E. (2011). HSP90 functions in the circadian clock through stabilization of the client F-box protein ZEITLUPE. Proc. Natl. Acad. Sci. USA **108:** 16843–16848.

Kim, W.Y., Geng, R., and Somers, D.E. (2003). Circadian phase-specific degradation of the F-box protein ZTL is mediated by the proteasome. Proc. Natl. Acad. Sci. USA **100:** 4933–4938.

Krishna, P., and Gloor, G. (2001). The Hsp90 family of proteins in *Arabidopsis thaliana.* Cell Stress Chaperones **6:** 238–246.

Lata, C., and Prasad, M. (2011). Role of DREBs in regulation of abiotic stress responses in plants. J. Exp. Bot. **62:** 4731–4748.

Lee, D.H., and Goldberg, A.L. (1998). Proteasome inhibitors: valuable new tools for cell biologists. Trends Cell Biol. **8:** 397–403.

Lee, S., Lee, D.W., Lee, Y., Mayer, U., Stierhof, Y.D., Lee, S., Jürgens, G., and Hwang, I. (2009). Heat shock protein cognate 70-4 and an E3 ubiquitin ligase, CHIP, mediate plastid-destined precursor degradation through the ubiquitin-26S proteasome system in *Arabidopsis.* Plant Cell **21:** 3984–4001.

Lee, S., Seo, P.J., Lee, H.J., and Park, C.M. (2012). A NAC transcription factor NTL4 promotes reactive oxygen species production during drought-induced leaf senescence in *Arabidopsis.* Plant J. **70:** 831–844.

Marcolino-Gomes, J., Rodrigues, F.A., Fuganti-Pagliarini, R., Bendix, C., Nakayama, T.J., Celaya, B., Molinari, H.B., de Oliveira, M.C., Harmon, F.G., and Nepomuceno, A. (2014). Diurnal oscillations of soybean circadian clock and drought responsive genes. PLoS One **9:** e86402.

Martin-Tryon, E.L., Kreps, J.A., and Harmer, S.L. (2007). GIGANTEA acts in blue light signaling and has biochemically separable roles in circadian clock and flowering time regulation. Plant Physiol. **143:** 473–486.

Más, P., Kim, W.Y., Somers, D.E., and Kay, S.A. (2003). Targeted degradation of TOC1 by ZTL modulates circadian function in *Arabidopsis thaliana.* Nature **426:** 567–570.

McClellan, A.J., Tam, S., Kaganovich, D., and Frydman, J. (2005). Protein quality control: chaperones culling corrupt conformations. Nat. Cell Biol. **7:** 736–741.

Meiri, D., and Breiman, A. (2009). *Arabidopsis* ROF1 (FKBP62) modulates thermotolerance by interacting with HSP90.1 and affecting the accumulation of HsfA2-regulated sHSPs. Plant J. **59:** 387–399.

Norén, L., Kindgren, P., Stachula, P., Rühl, M., Eriksson, M.E., Hurry, V., and Strand, Å. (2016). Circadian and plastid signaling pathways are integrated to ensure correct expression of the CBF and COR genes during photoperiodic growth. Plant Physiol. **171:** 1392–1406.

Panchuk, I.I., Volkov, R.A., and Schöffl, F. (2002). Heat stress- and heat shock transcription factor-dependent expression and activity of ascorbate peroxidase in *Arabidopsis.* Plant Physiol. **129:** 838–853.

Rensing, L., Bos, A., Kroeger, J., and Cornelius, G. (1987). Possible link between circadian rhythm and heat shock response in *Neurospora crassa*. Chronobiol. Int. **4:** 543–549.

Samant, R.S., Clarke, P.A., and Workman, P. (2014). E3 ubiquitin ligase Cullin-5 modulates multiple molecular and cellular responses to heat shock protein 90 inhibition in human cancer cells. Proc. Natl. Acad. Sci. USA **111:** 6834–6839.

Sangster, T.A., Salathia, N., Lee, H.N., Watanabe, E., Schellenberg, K., Morneau, K., Wang, H., Undurraga, S., Queitsch, C., and Lindquist, S. (2008). HSP90-buffered genetic variation is common in *Arabidopsis thaliana.* Proc. Natl. Acad. Sci. USA **105:** 2969–2974.

Sangster, T.A., and Queitsch, C. (2005). The HSP90 chaperone complex, an emerging force in plant development and phenotypic plasticity. Curr. Opin. Plant Biol. **8:** 86–92.

Schneider, R., Linka, R.M., and Reinke, H. (2014). HSP90 affects the stability of BMAL1 and circadian gene expression. J. Biol. Rhythms **29:** 87–96.

Seo, P.J., Park, M.J., Lim, M.H., Kim, S.G., Lee, M., Baldwin, I.T., and Park, C.M. (2012). A self-regulatory circuit of CIRCADIAN CLOCK-ASSOCIATED1 underlies the circadian clock regulation of temperature responses in *Arabidopsis.* Plant Cell **24:** 2427–2442.

Shirasu, K. (2009). The HSP90-SGT1 chaperone complex for NLR immune sensors. Annu. Rev. Plant Biol. **60:** 139–164.

Tamaru, T., Hattori, M., Ninomiya, Y., Kawamura, G., Varès, G., Honda, K., Mishra, D.P., Wang, B., Benjamin, I., Sassone-Corsi, P., Ozawa, T., and Takamatsu, K. (2013). ROS stress resets circadian clocks to coordinate pro-survival signals. PLoS One **8:** e82006.

von Koskull-Döring, P., Scharf, K.D., and Nover, L. (2007). The diversity of plant heat stress transcription factors. Trends Plant Sci. **12:** 452–457.

Wang, X., Li, X., and Li, Y. (2007). A modified Coomassie Brilliant Blue staining method at nanogram sensitivity compatible with proteomic analysis. Biotechnol. Lett. **29:** 1599–1603.

Xu, Z.S., Li, Z.Y., Chen, Y., Chen, M., Li, L.C., and Ma, Y.Z. (2012). Heat shock protein 90 in plants: molecular mechanisms and roles in stress responses. Int. J. Mol. Sci. **13:** 15706–15723.

Yamamoto, Y., Sato, E., Shimizu, T., Nakamich, N., Sato, S., Kato, T., Tabata, S., Nagatani, A., Yamashino, T., and Mizuno, T. (2003). Comparative genetic studies on the APRR5 and APRR7 genes belonging to the APRR1/TOC1 quintet implicated in circadian rhythm, control of flowering time, and early photomorphogenesis. Plant Cell Physiol. **44:** 1119–1130.

Yoo, C.Y., Miura, K., Jin, J.B., Lee, J., Park, H.C., Salt, D.E., Yun, D.J., Bressan, R.A., and Hasegawa, P.M. (2006). SIZ1 small ubiquitin-like modifier E3 ligase facilitates basal thermotolerance in *Arabidopsis* independent of salicylic acid. Plant Physiol. **142:** 1548–1558.

Yoo, S.D., Cho, Y.H., and Sheen, J. (2007). Arabidopsis mesophyll protoplasts: a versatile cell system for transient gene expression analysis. Nat. Protoc. **2:** 1565–1572.

Yoo, Y.S., et al. (2015). The mitochondrial ubiquitin ligase MARCH5 resolves MAVS aggregates during antiviral signalling. Nat. Commun. **6:** 7910.

Zhou, J., Wang, J., Cheng, Y., Chi, Y.J., Fan, B., Yu, J.Q., and Chen, Z. (2013). NBR1-mediated selective autophagy targets insoluble ubiquitinated protein aggregates in plant stress responses. PLoS Genet. **9:** e1003196.

Zhou, J., Zhang, Y., Qi, J., Chi, Y., Fan, B., Yu, J.Q., and Chen, Z. (2014). E3 ubiquitin ligase CHIP and NBR1-mediated selective autophagy protect additively against proteotoxicity in plant stress responses. PLoS Genet. **10:** e1004116.